

Original Article

Hybrid Nanofluid-Assisted Minimum Quantity Lubrication (MQL) for Turning AISI 1040 Steel (EN8): An Experimental and Machine Learning Approach

Dattatraya Popat Kshirsagar¹, Amol Dnyanwshwar Wable², Swapnil Dnyadeo Galande³, Atul Bhausaheb Pawar⁴, Vishnu Damodhar Wakchaure⁵

¹Department of Mechanical Engineering, SNDCOE RC Yeola, SPPU Pune University, Maharashtra, India.

²Department of Mechanical Engineering, SCOE Kopergaon, SPPU Pune University, Maharashtra, India.

^{3,5}Department of Mechanical Engineering, AVCOE Sangamner, SPPU Pune University, Maharashtra, India.

⁴Department of Electrical Engineering, SNDCOE & RC Yeola, SPPU Pune University, Maharashtra, India.

¹Corresponding Author : dattatrayakshirsagar07@gmail.com

Received: 01 January 2026

Revised: 08 February 2026

Accepted: 10 March 2026

Published: 29 April 2026

Abstract - The study presents an experimental and predictive investigation of bio-degradable nanofluids for sustainable machining under Small Quantity Lubrication (SQL). Palm oil, selected for its biodegradable and eco-friendly characteristics, was blended with Silicon Carbide (SiC), Titanium Dioxide (TiO₂), and their hybrid mixtures at different concentrations. Turning tests were carried out on AISI 1040 (EN8) steel using a Taguchi L27 design, covering 81 trials with varying surface speed, feed rate, radial depth of cut, and nanofluid parameters. Adding the nanoparticles improves thermal conductivity, viscosity, and stability of the nano fluid, showing the machining efficiency and Material Removal Rate (MRR). To predict MRR, Artificial Neural Networks (ANN) and multiple deep learning techniques were used. The decision Tree, Support Vector Regression, Random Forest, AdaBoost, XGBoost, Gradient Boosting, and CatBoost were implemented. Among them, ensemble learning methods such as Gradient Boosting ($R^2 = 0.9944$) and XGBoost ($R^2 = 0.9876$) demonstrated the highest accuracy, while ANN also achieved strong generalization ($R^2 = 0.9598$). The results confirm that hybrid nanofluid-based MQL significantly improves machining sustainability and that ensemble machine learning approaches provide reliable prediction of machining performance.

Keywords - Minimum Quantity Lubrication, Hybrid Nanoparticles, Machine Learning Models, Predictive Modeling, Small Quantity Lubrication.

1. Introduction

Cutting fluids limit the rise in temperature within the machining zone by establishing a protective lubricating boundary that lowers friction within the cutting zone's interfacial boundaries. They also reduce mechanical stress on the cutting tool by facilitating chip separation from the cutting area. Owing to these physical and chemical characteristics, cutting fluids are indispensable in machining processes, as they mitigate thermal and mechanical degradation of the cutting tool and the substrate. Despite these benefits, it is well recognized that many cutting fluids, particularly those formulated with chemical additives, pose a potential risk to the environment and human health.

Moreover, the financial outlays required for their procurement, maintenance, and treatment of contaminated lubricants contribute substantially to overall manufacturing expenses [1].

Minimum Quantity Lubrication (MQL) improves machining performance by supplying a very small amount of lubricant combined via a high-velocity mist impinging directly upon the primary deformation zone. This aerosol delivery allows better penetration at the tool-workpiece interface than Conventional Cutting Fluids (CCF), thereby enhancing lubrication and cooling efficiency. Due to its low lubricant consumption, MQL is considered a sustainable machining technique, as it reduces operational costs and mitigates environmental and health concerns. To further advance the effectiveness of MQL, current research focuses on the development of Nanofluid-based MQL (NMQL) systems.

In NMQL, nanoparticles are dispersed within the base lubricant to exploit their superior thermo-physical properties, facilitating accelerated thermal dissipation, attenuated interfacial friction, and superior machining characteristics compared to conventional MQL [2].



Table 1. Studies using different nanofluids in assisted machining processes

Machine	Workpiece	Tool	Nanofluids	Base oil	Surfactants	Ref.
Turning	AISI 304 steel	carbide	SiO ₂	sunflower oil	Sodium Dodecyl Sulfate	[1]
Slot milling	Ti-6Al-4V	carbide	Al ₂ O ₃ and CuO	polymeric ester-based oil	no	[2]
Srinding	Ti-6Al-4V titanium alloy and ZrO ₂ ceramic	diamond wheel	graphene and Al ₂ O ₃	oleic acid	no	[3]
Drilling	Nickel-based hasten alloy C276	TiN-coated carbide drill bit	graphene and Al ₂ O ₃	water based	sodium dodecyl sulfate	[4]
Grinding	Ti-6Al-4V alloy	diamond wheel	graphene nanoplatelets	distilled water (ethanol)	Sodium deoxycholate	[6]
Turning	Nickel-based hasten alloy C276	carbide	graphene	canola oil	no	[7]
Turning	austenitic AISI 310 S SS	TiCN-coated	nMoS ₂ and ngraphene	Erroil KT/2000	no	[8]
Micromilling	TC4 titanium alloy	diamond tool	graphene	water based	no	[9]
Milling	CGI cast iron	carbide insert	nMoS ₂ and MWCNT	Erroil KT/2000	sodium dodecyl sulfate	[10]
Milling	Waspaloy superalloy	cemented carbide	CuO and ZnO	sunflower oil	GA,SDS,CTAB, and PVP	[11]
Micromilling	Ti6Al4V alloy	WC with AlTiN coating	CuO and MoS ₂	soybean oil	no	[12]
Milling	titanium alloy	cemented carbide	C60	water based	no	[13]
Microtexture	stainless steel 316 L	cermet	Fe ₃ O ₄	water based	oleic acid	[14]
Turning	hardened steel	ceramic	SiC	rapseed oil, castor oil	no	[15]
Turning	90CrSi steel	CBN inserts	Al ₂ O ₃ , MoS ₂	Soybean oil	no	[16]
Turning	inconel 625	PVD TiAlN-coated	MoS ₂ and graphite	sunflower oil	no	[17]
Turning	Haynes 25 superalloy	cermet	N ₂ gas and graphene nanoplatelet, multiwalled carbon nanotubes	Plantocut 10 SR oil	no	[18]
Turning	Ti6Al4V alloy	TiC ceramic	Fe ₃ O ₄ and CNTs	deionised water	no	[19]
Turning	compacted graphite iron	AlNTi coating tools	MQL, LN ₂	M 106 cutting oil	no	[20]
Turning	Ti6Al4V alloy	TiAlN-coated inserts	halogenated IIs	canola oil	tween 80	[21]

Milling	SA508-3 steel	no	scCO ₂ -MQL	no	no	[22]
Milling	TA2 pure titanium	solid carbide	no	castrol syntilo 9930C and Blasocut 2000CF	no	[23]
Milling	AMS 5704 Waspaloy	Stainless steel 316	no	water based	no	[24]
Grinding	nimonic 80A	no	no	Ionic liquid with rice bran oil	no	[25]

The addition of relevant volumetric values of nano-additives to the medium can greatly enhance tribological efficiency and thermal transport properties. The addition of nanoparticles enhances the adsorption layer in interfaces in contact with each other. Moreover, the existence of nanoparticles can increase micro-scale agitation in the medium, thus significantly increasing the thermal transport coefficient to enhance efficient heat dissipation. Researchers in recent times have begun employing a hybrid form of nano-suspension in many subtractive manufacturing techniques. A notable volume of literature has been established to explore the influence of various nano-particulates in conventional carrier fluids with respect to modulation in thermo-physical properties, as well as friction reduction potential. The improvement in thermal conductivity is influenced by various factors, including geometric structure and sizes, volumetric concentration, level of dispersion, and inherent thermal properties [3].

These nanofluids have been identified as a colloidal suspension of nano-scale particulates (i.e., less than 100 nm) engineered within a continuous oil or alcohol liquid carrier medium. Different concentrations of graphene and Al₂O₃ nanoparticles were shown by Panigrahi to be utilized to prepare the nano and bio-degraded hybrid nanofluids, which were used for mist cooling when utilized for the Hastelloy C276 drilling process. As a result, a combination of these two nanoparticles gives a synergistic effect that enhances the inner surface topography of a hole created by a drill bit. [4].

Traditional metalworking fluids are mainly formulated from petroleum-based mineral oils and often contain additives that are toxic, carcinogenic, non-biodegradable, and environmentally unsustainable; thus, they pose severe risks to ecological systems and the health of operators. By contrast, vegetable lubricants have a more benign environmental profile due to their biodegradable, renewable sources. They possess several other technical advantages, such as higher flash points, increased viscosity, improved lubricity, better tribological performance than mineral oils, and reduced evaporative losses. However, their full applications have been greatly limited by the poor thermal and oxidative stability, higher costs, food-versus-energy utilization issues, and poor low-

temperature fluidity. Currently, the above disadvantages of vegetable-based oils have been overcome by developing nanoparticle-enhanced cooling and lubrication fluids by dispersing engineered nanoparticles into vegetable-based oils. It improved the thermal properties of nanofluids and extended applications in the field of material processing and machining operations [5]. Table 1 presents the applications of different types of nanofluids, base oils, and surfactants during various machining operations, such as drilling, milling, turning, and grinding, on workpiece materials with different types of cutting tool inserts.

Previously, machine learning technology has been used in the prediction and optimization of important responses related to tool wear kinetics, surface topography, thermal gradients, and volumetric rates. It can be carried out through supervised and unsupervised learning. In Supervised Learning (SL), models are trained on datasets containing features (independent parameters) and labels (dependent parameters, such as MRR). Alternatively, Unsupervised Learning (UL) manages unlabelled information, utilizing computational architectures to uncover underlying clusters and correlations without external guidance. Among these, Artificial Neural Networks (ANN) are particularly effective in handling complex problems with many trainable parameters. State-of-the-art connectionist models, encompassing convolutional and recurrent architectures, have also been explored to improve prediction accuracy in manufacturing and process optimization tasks [26].

Stemmer et al. developed several connectionist models (ANNs) and performed a comparative assessment of their performance with a regression-based approach for predicting the flank wear land width using recorded machining forces as input variables. By varying the training and testing datasets, their findings demonstrated superior extrapolation capability when prior knowledge was incorporated, compared to conventional ANN models without such information [26]. Liu et al. successfully predicted cutting tool temperature, an analytical parameter for prolonging tool life or maintaining workpiece quality. Excessive heat generation during metal cutting adversely affects machining performance by accelerating thermally induced tool wear and introducing unfavorable tensile residual stresses in the machined surface.

The hybrid modeling approach incorporated a neural network-based regression framework to estimate both cutting forces and thermal tool loads. Nevertheless, differences greater than 15% were found between the predicted and experimental values for tool heat transfer [27]. Ouerhani et al. utilized a computational modeling strategy to map and anticipate thermal deformations, enabling adjustment of the tool reference position. Four stochastic and deterministic modeling techniques, encompassing linear-based regression and tree-based hierarchical learning, MLP Regress, and Elastic Net, were trained on a portion of the experimentally acquired dataset and verified utilizing the unseen test partition. Among these, three algorithms achieved a Mean Absolute Error (MAE) below 1 μm along with correlation coefficients exceeding 90% [28].

Khoshaim et al. developed two hybrid computational neural frameworks utilizing experimental training sets to model the stochastic nature of process outputs. The prediction capability of these models was further improved by integrating metaheuristic optimization techniques, specifically (PSO) and the (FPA) [29]. Trujillo et al. designed a shallow feed-forward ANN to model morphological deviations from the design specification during dry turning of AA7075 (Al-Zn) alloy, achieving adjusted R^2 values in the range of 0.87–0.97 across all considered variables [30]. Abeni et al., in their analysis of tool wear in the turning of AISI 1045 steel, have presented a reliable way to predict tool life when cutting speed fluctuates [31].

Laakso et al. justified the use of a hybrid Finite Element Machine Learning (FEML) approach for simulating metal cutting processes. In their proposed FEML approach, the authors employed the Coupled Eulerian-Lagrange (CEL) formulation and used Tensor Flow. Compared to using DNN or FEM independently, the hybrid FEML model delivered better performance by lowering computational time, and there are alternative ways to describe reducing the average prediction error from 23% to 13% [32]. Zhu et al. carried out a method for in-process prediction and autonomous evaluation of surface integrity indices. Among several models assessed, including k-NN, Decision Trees, Support Vector Regression (SVR), Gradient Boosted Regression (GBR), Random Forests (RF), Extra Trees (ET), and ANN, the SVR and k-NN models achieved the highest prediction accuracy and the least uncertainty across all signal processing techniques [33]. Saikrupa et al. formulated an SVM-driven prognostic framework for the estimation of surface finish, providing an empirical basis for analyzing process performance. The model showed strong reliability, with R^2 indices of 0.87 and 0.90 for the forecasting of power requirements and surface topography, respectively [34].

Srivastava et al. show that a dual-architecture Adaptive Neuro-Fuzzy Inference System, configured as a pair of Multi-Input Single-Output (MISO) frameworks, estimates tool

degradation mechanisms and the resulting surface topography during CNC turning of CFRP using a coated carbide tool. The developed models demonstrated excellent predictive performance, with close agreement between predicted and experimental values, achieving accuracies of 98.96% for tool wear and 99.61% for surface roughness [35]. In a different study, Geibel et al. employed an MCMC-based Bayesian inference method to estimate the posterior distributions of cutting force model parameters.

The parameters estimated by employing the simple face-turning experiment were useful to predict cutting forces under different tool-workpiece engagement conditions [36]. Li et al. introduced a prognostic methodology for estimating residual stress profiles during the heavy-duty turning of Ti-6Al-4V, incorporating cutting temperature and cutting force as inputs. The proposed model demonstrated strong accuracy, with relative errors below 6% when comparing predicted and simulated residual stress values, confirming its effectiveness in stress analysis [37]. Jacob et al. developed an accurate and robust predictive model for surface roughness after finishing turning operations. The proposed approach employs a model ensemble method, which combines multiple predictive models, SVM, GB, ADA, CAT, GPR, RF, VR, SR, to improve the precision of the predictions. The Voting Regressor Ensemble achieved a 5.65% increase in demonstrated predictive efficacy relative to the most robust standalone architecture [38].

In this research work, palm oil-based cutting fluid was formulated with the addition of Silicon Carbide (SiC), Titanium Dioxide (TiO₂), and their hybrid combination as nano-materials. Turning experiments were performed on AISI 1040 steel, and the Material Removal Rate (MRR) was recorded for 81 samples. The collected data were analyzed using Artificial Neural Networks (ANN) along with seven different machine learning algorithms to synthesize data-driven estimators for process optimization. The estimation accuracy of the paradigms was rigorously scrutinized through standard performance metrics to compare their effectiveness in predicting MRR.

2. Materials and Methods

Palm oil was selected as a biodegradable base fluid for this machining study for several reasons. Earlier studies have shown that palm oil provides superior surface finishes compared with mineral oil and offers greater tool life than other bio oils. The physicochemical properties of the palm-based oil used for this investigation are outlined in Table 2. In addition to improving lubricity, nanoparticles were evaluated as oil additives. A review of literature revealed that SiC and TiO₂ nano-materials are very efficient in retaining their thermal and physical properties when blended with vegetable-based oils, especially palm oil. The oils were chosen for this investigation owing to the expectation of high temperatures generated during the machining process.

Table 2. Chemical and physical characteristics of palm oil

Parameter	Value
Temperature (°C)	20 to 298
Viscosity (MPa·s)	119.99
Heat Capacity (kJ/kg·°C)	1.748 to 2.858
Thermal Conductivity (W/m·K)	0.121
Volumetric mass (kg/m ³)	891.1 to 778.9
Calorific Value (MJ/kg)	37.000 to 37.900
Flash Point (°C)	103
Thermal Resistivity (cm·K/W)	829.3
Fire point (°C)	250 to 301

In this research, hybrid nano-fluids were synthesized via the two-step method of nano-fluid preparation. The palm oil was utilized as a major base fluid in dispersing both (SiC) nanoparticles and (TiO₂). The concentration levels utilized were volumetric percentages of 1%, 2%, and 3%. The SDS surfactant was utilized as a stabilizing agent in controlling nanoparticle agglutination and ensuring homogeneity in the nano-fluids. The two-step procedure utilized in this research is attributed to being most widely utilized in machining research for formulating nano-fluids. In this procedure, nano-materials, including nanoparticles, nanofibers, or nanotubes, are synthesized in powder form using either a physical or a chemical method in the first step. The second step utilizes homogeneity in mixing these nanopowders with their respective nano-fluids using any of the mixing techniques, high-shear mixing, ball milling, magnetic mixing, ultrasonic mixing, and homogenization. The prepared hybrid nano-fluid samples are presented in Figure 2.

Table 3. Properties of various samples

Sample Vol. %	Density (g/cm ³)	Viscosity (MPa·s)	Calorific Value (MJ/kg)	Flash Point (°C)	Thermal Conductivity (W/m·K)	Thermal Resistivity (cm·K/W)
Palm oil (Base fluid)	0.859	119.99	37.000	103	0.121	829.3
Palm oil + SiC (1%)	0.858	1.023	37.500	105	0.118	846.4
Palm oil + SiC, (2%)	0.859	1.435	37.800	109	0.107	934.7
Palm oil + SiC, (3%)	0.859	1.567	37.800	111	0.135	699.2
Palm oil + TiO ₂ , (1%)	0.857	49.32	37.500	107	0.119	842.6
Palm oil + TiO ₂ , (2%)	0.858	10.32	37.660	105	0.132	756.8
Palm oil + TiO ₂ , (3%)	0.860	10.55	37.790	113	0.116	897.5
Palm oil + SiC+TiO ₂ , (1%)	0.859	10.74	37.600	106	0.126	791.6
Palm oil + SiC+TiO ₂ , (2%)	0.858	10.56	37.690	110	0.134	1008
Palm oil + SiC+TiO ₂ , (3%)	0.858	50.05	37.900	113	0.147	678.7

The evolution of the physical and thermal properties of the base lubricant with the integration of SiC and TiO₂ nano-additives can be cataloged as shown in Table 3. The addition of SiC and TiO₂ nano-additives enhances its thermal conductivity and flash points. A significant increase in viscosity could affect fluid flow behavior, particularly at higher nanoparticle concentrations.

**Fig. 1 Prepared samples of hybrid nanofluid**

This work focuses on turning of AISI 1040 steel for the purpose of improving machining productivity and surface quality under MQL. The machining experiments were conducted on a high-precision CNC machining center, where a CNC Fanuc Series OI Mate-TB) with the set-up of the MQL system.

The MQL arrangement was developed for the optimum of lubrication cooling, and lubricant feeding was controlled through a spray gun (40 ml/min with an atomization pressure of 3 bar). Critical output parameters such as temperature at the cutting zone, surface roughness of the processed specimen, and Material Removal Rate (MRR) were systematically ascertained to analyse the machining performance.

These parameters were selected to assess the thermal, dimensional, and productivity aspects of the process. The figure shows the turned samples of AISI 1040 steel using palm oil with nanolubricants.



Fig. 2 Hybrid nano-fluid samples



Fig. 3 Turned samples of AISI 1040 steel

Table 4. Input variables in MQL machining test

Parameter	Unit	Values
Cutting Speed	RPM	700, 1000, 1300
Feed Rate	mm/rev	0.1, 0.15, 0.2
Depth of cut	mm	0.8, 0.9, 1
Volume Concentration	%	1, 2, 3
Material	-	SiC, TiO ₂ , Hybrid (SiC+TiO ₂)

Table 5. Parametric configuration and observed surface integrity metrics for SiC, TiO₂, and combined (SiC+TiO₂)

Sr. No.	Cutting speed, rpm	Feed rate, mm/rev	Depth of cut, mm	Volume, %	Nano Material	MRR, mm ³ /min
1	700	0.1	0.8	1	SiC	5850
2	1000	0.2	0.8		SiC	12289
3	1300	0.2	1.0		SiC	22659
4	1000	0.1	0.8	2	SiC	7658
5	1300	0.2	0.8		SiC	13258
6	700	0.2	1.0		SiC	24358
7	1300	0.1	0.8	3	SiC	7030
8	700	0.2	0.8		SiC	15357
9	1000	0.2	1.0		SiC	28354
10	700	0.1	0.8	1	TiO ₂	5766
11	1000	0.1	1.0		TiO ₂	11765
12	1300	0.2	1.0		TiO ₂	20845
13	1000	0.1	0.8	2	TiO ₂	7078
14	1300	0.2	0.8		TiO ₂	12674
15	700	0.2	1.0		TiO ₂	23457
16	1300	0.1	0.8	3	TiO ₂	6389

A two-level CCD was used to study and analyze the effect of some process parameters on (MRR), as presented in Table 4. (water-based) Minimum Quantity Lubrication (MQL) of grinding neat oil with biodegradable nanofluids. Cutting speed was taken at three levels (700, 1000, and 1300 RPM), feed rate at 0.10, 0.15, and 0.20 mm/rev., and depth of cut at 0.8, 0.9, and 1.0 mm in order to cover low, medium, as well as high machining conditions.

With nanoparticle concentrations of 1%, 2%, and 3%, palm oil was used as the base fluid to create the lubricant. Titanium dioxide (TiO₂), Silicon Carbide (SiC), and a hybrid blend of both nano-material conditions were examined. These parameter levels were chosen to offer a variety of lubricant formulas and machining circumstances, allowing for a thorough assessment of their impact on MRR and making it easier to build high-fidelity prognostic structures.

In a total of 81 experiments, an analysis of the effects of machining and lubrication factors on volumetric Material Removal Rate (MRR) in processes involving turning with minimal quantity lubrication was done. The experiments were conducted in accordance with the Taguchi design L27. The Taguchi design offers a highly organized and efficient mode to run experiments involving numerous parameters. The investigation included five unique processing parameters: CS, FR, DOC, concentration, and type of nano-materials.

For each nano-material, 27 experiments were conducted, resulting in a total of 81 experiments. All experiments were conducted on a conventional lathe. The output variable, MRR, was experimentally recorded for each experiment. The results have greatly reduced the number of trials needed to obtain a range of data, thus making a reliable set of data to build a model. Table 6 is a summary of the output variable, MRR.

17	700	0.2	0.8		TiO2	14038
18	1000	0.2	1.0		TiO2	26087
19	700	0.1	0.8	1	SiC+TiO2	5892
20	1000	0.1	1.0		SiC+TiO2	12398
21	1300	0.2	1.0		SiC+TiO2	22812
22	1000	0.1	0.8	2	SiC+TiO2	7691
23	1300	0.2	0.8		SiC+TiO2	13321
24	700	0.2	1.0		SiC+TiO2	24572
25	1300	0.1	0.8	3	SiC+TiO2	7082
26	700	0.2	0.8		SiC+TiO2	15452
27	1000	0.2	1.0		SiC+TiO2	28618

Table 6. Process characteristics in MQL testing

Parameter	Min	Max	Mean	SD
MRR	5766	28618	14267.16	5508.16

3. Pre-Processing of the Dataset

For pre-processing, Pandas was used for data handling and organization, while scikit-learn provided pre-processing tools such as binary expansion of categorical attributes alongside the standardization of numerical inputs. To enable an impartial evaluation of the model's capacity for generalization, the experimental dataset was divided into distinct training and testing subsets. This property was converted into a binary vector representation using One-Hot Encoding, which was carried out using the Scikit-learn framework in order to account for the categorical nature of the nano-material kind.

This technique creates separate binary columns for each material (SiC, TiO₂, and Hybrid), ensuring that the ANN can process the information without introducing artificial ordinal relationships. The encoded features were then merged with the original dataset to form the final input matrix used for model training.

Outlier analysis was done on the experimental dataset using a box plot for MRR. The box plot showed that all data points fall within the interquartile range, meaning there are no significant outliers. This supports the reliability of the collected experimental readings. It allows us to keep all values for further analysis and model training without needing to clean or remove any data. For ANN modeling, the dataset was divided into input features: cutting speed, feed rate, depth of cut, nanofluid concentration, and nano-material type, after one-hot encoding. The target variable was MRR. This division ensured that the model could accurately represent the non-linear relationships between input machining parameters and lubrication variables in relation to the resulting MRR. All input features were normalized using the Standard Scalar method from Scikit-learn to eliminate scaling issues among variables measured in different units, such as cutting speed (RPM), feed rate (mm/rev), and nanoparticle concentration (%). After scaling the features, the observations were split into training and verification groups using an 80:20 ratio, with a

set random state to ensure consistent findings. The training group was used to build and adjust the ANN model, while the testing group measured estimation accuracy on previously unseen observations.

3.1. ANN Model

The ANN model was built using the Keras/Tensor Flow environment with a Sequential constructor that enables modular (one layer at a time) construction of models. The number of preprocessed features determined the input layer. The model consisted of four Intermediate latent layers: the first layer had 128 perceptrons with a tanh activation function that helped in achieving smooth gradient flow and could accommodate positive as well as negative input values. The next 3 layers contained 64, 32, and 16 perceptrons, as the activation of each was with the ReLU function to capture non-linear dependencies while mitigating vanishing gradient problems. The architecture ends with a single linear output unit that is designed to directly map the high-level features generated by the hidden layers into a continuous numerical value representing MRR.

To formulate the computations implemented by neuron n_2 in a mathematical sense, first, the perceptron output is defined as the weighted sum of its input signals (1)

$$n = \sum_{i=1}^p (W_i X_i + b) \quad (1)$$

Where W_i is the associated synaptic weights, X_i for input values, p for the number of total inputs, and b for the bias term. The final activation state of the node is determined by applying a non-linear transformation to the sum of the weighted input and the associated bias. The above output of the neuron can be formulated in the mathematical form as we denoted by a non-linear activation function $f(n)$. [40]:

$$f(n) = f\left(\sum_{i=1}^p (W_i X_i + b)\right) \quad (2)$$

Since the primary task of models was regression-oriented, MSE (Mean Squared Error) was chosen as the loss function, and for optimization, the Adam optimizer, known for its good enough adaptive learning rate property, was employed. Also, in order to enhance the intuitiveness of estimation

dependability, Mean Absolute Error (MAE) as a performance statistical criterion was utilized.

The network was trained using 100 epochs and a mini-batch size of 5, with a training/validation split of 80/20. The performance of the model was followed during both the training phase and validation phase by monitoring errors, to guarantee the convergence and avoid over-fitting or under-fitting during training.

The deep learning regressor developed in this study, as seen in Figure 4, is made up of an input layer of 7 nodes representing the machining and nanofluid parameters, which is followed by 4 perceptron layers. The largest hidden layer has a density of 128 number crunching nodes, employing the hyperbolic tan operator to normalize the activations to a $[1,1] [-1,1]$ range, and is used to successfully model positive as well as negative relations in the data. The first layer in the generator is Since the \tanh operator is zero-centered, we get faster gradient descent and robust saturation control over the entire input domain. The $\tanh(x)$ function of the hyperbolic tangent can be mathematically defined as [40]

$$\tanh(x) = \frac{e^x - e^{-x}}{e^x + e^{-x}} \quad (3)$$

Application of ReLU activation functions allows for non-linear mapping functions to be learned, which are extremely fast converging relative to typical saturating activation functions, and allow for the mitigation of the vanishing gradient problem, leading to faster converging networks. The final layer exists with only a single output node (which employs an identity activation function) in order to project the high-dimensional space into a single continuous estimate of the MRR. Thus, the hierarchy of such a construction allows the network to learn progressively complicated, highly non-linear functional mappings between the input machining parameters and the MRR.

3.2. Single Model

Decision Tree Regressor was used to model the MRR based on the machining and nanofluid parameters. The algorithm constructs a binary decision tree by recursively subdividing the feature space into more and more similar regions according to the best possible split function. Each internal node in the hierarchy specifies a test on an input parameter, while each terminal node delivers the output value. The architecture was optimized using a parameter search on the hyperparameter space by a randomized search in conjunction with cross-validation, searching for the best combination of Structural depth, Internal node threshold, and feature selection strategy. Support Vector Regression (SVR) was used to model the MRR based on machining parameters and nanofluid parameters. Click to humanize. The regression application of the SVR construct seeks to approximate a hyperplane that encloses the maximum number of training

samples within an epsilon-insensitive tube. Click to humanize To evaluate the kindred architecture, the hyperparameter scope of the cost coefficient, the kernel function, and the epsilon margin of tolerance for error was studied through a randomized search heuristic coupled with successive rounds of iteration.

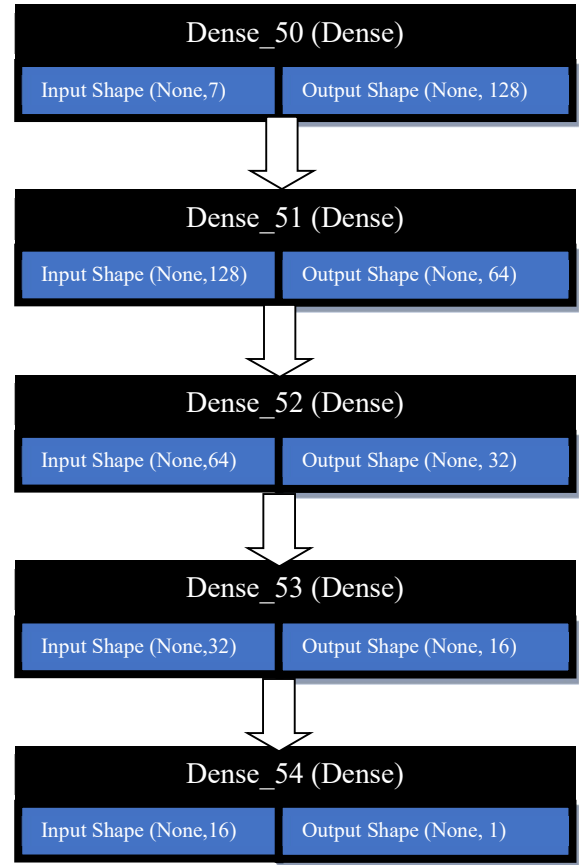


Fig. 4 ANN architecture

3.3. Ensemble Model

Random Forest Regression was applied to predict the MRR with an ensemble of decision trees. The random forest algorithm randomly injects an additional layer of stochastic variation compared to the classical bagging model by randomly selecting a feature subspace per split to ensure the base learners decorrelate from each other. The best hyperparameter configuration was determined by using the best combination of the Optimization iterations, Structural depth, internal node threshold, and Terminal node density. Click to humanize implementation of the model performed a systematic hyper-parameter search by tuning the serial iterations and structural depth, which minimizes the training error. This allows the model to generalize better when new samples are introduced. Adaptive Boosting (AdaBoost), where the elementary decision trees are integrated randomly over a recursive cascade, proved a useful prognostic tool for predicting the Material Removal Rate (MRR).

In AdaBoost, each new tree tries to bias the features it gets to make a better prediction. Each time the training error rate diminishes through iterations, the regressor learns better, and begins to bias the samples used for prediction more and more fairly. A Decision Tree Regressor with depth 3 was used as the base estimator, and Randomized Search CV was utilized to optimize hyperparameters defined by the Optimization iterations, Update velocity, and loss function (loss).

An XG Boost regression algorithm was used to predict the MRR due to its ability to model nonlinear interactions and

high-dimensional spaces efficiently. XGBoost is an implementation of gradient boosting tree and consists of a flexible sequential additive modeling strategy where each new tree built is optimized with respect to all effects it may have on the existing set of trees. For our problem, the model was fit with RandomizedSearchCV in order to optimize the following elements and their number of iterations: Optimization iterations, Update velocity, Structural depth, child weight, subsample ratio, feature sampling ratio, and regularization parameter (gamma).

Table 7. Algorithm settings for different models

Set	Type	Variable	Value
Single	Decision Tree	Structural depth	3
		Internal node threshold	4
		Terminal node density	3
		K-fold partitioning strategy	3
	SVM	C	1000
		Kernel	RBF
Ensemble	Random Forest	Optimization iterations	250
		Structural depth	30
		Internal node threshold	2
		Terminal node density	1
		K-fold partitioning strategy	3-fold
	AdaBoost	Optimization iterations	450
		Update velocity	0.45
		Structural depth	3
		Internal node threshold	2
		Terminal node density	1
		K-fold partitioning strategy	3-fold
	XGBoost	Optimization iterations	450
		Update velocity	0.12
		Structural depth	11
		Internal node threshold	1
		K-fold partitioning strategy	3-fold
	Gradient Boost	Optimization iterations	30
		Update velocity	0.2
		Structural depth	5
		Internal node threshold	5
		K-fold partitioning strategy	3
	Cat Boost	Optimization iterations	200
		Update velocity	0.1
		Structural depth	3
K-fold partitioning strategy		3	

Gradient Boosting Regression (GBR) was employed as one of the ensemble learning techniques to predict the MRR. By employing a first-order optimization technique, GBR progressively enhances its predictive fidelity. It accomplishes this by fitting new tree-based structures to the residuals, effectively descending along the error gradient to reach an optimal convergence point. This approach enabled the successful structuring of multi-variable models with high accuracy among the forecasting engines.

The performance of the different models was enhanced by utilizing a best-first search intensification strategy (via RandomizedSearchCV), essentially defined on a multi-dimensional hyper-parameter space. This optimization was primarily directed to the Selection iterations (n_estimators), gradient magnitude step size, model configuration related to Structural depth, and node partitioning limits.

The framework front-end adopts an iterative enhancement strategy, sequentially comprising a decision tree that is constructed by being specifically associated with the gradient of the cost function. The ability of the learning framework was also measured by employing a multi-metric of estimation, namely the MSE, MAE, MAPE, and R2, as displayed in the respective equations [40]

$$MSE = \frac{1}{m} \sum_{i=1}^m (P_i - T_i)^2 \quad (4)$$

$$MAE = \frac{1}{m} \sum_{i=1}^m |P_i - T_i| \quad (5)$$

$$R^2 = \frac{\sum_{i=1}^m (P_i - \bar{T})^2}{\sum_{i=1}^m (P_i - \bar{T})^2} \quad (6)$$

Where m is the total number of data points, P_i is the predicted value, T_i is the actual observed value, and T̄ is the mean of the actual values. Table 7 outlines the refined hyperparameters established for each learning paradigm via a systematic cross-validation approach, ensuring fair comparison and improved predictive performance.

4. Results and Discussion

The training performance of the implemented multilayer perceptron structure during training is illustrated in a schematic form in Figure 5, which depicts the change in loss versus the number of epochs. The training loss of the model decreases monotonically during the first phase of the iterations, and then reaches a quintessential state of convergence as training progresses. The MAE is at an ideal level during the training phase of the model.

The monotonous trend of loss and MAE validates that the proposed ANN architecture has the ability to extract the non-linear relationships of the entire dataset without underfitting and overfitting.

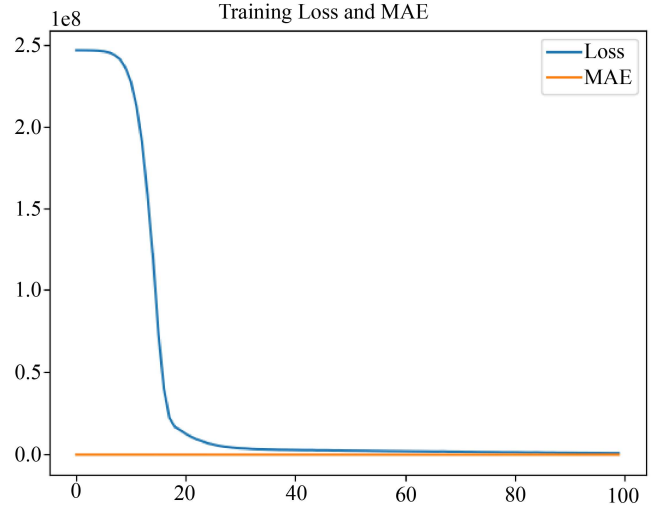


Fig. 5 Learning dynamics of the implemented computational framework

It is clear that different algorithms perform differently when comparing predictive models using R2, MSE, and MAE. The Gradient Boosting and Extreme Gradient Boosting frameworks outperformed all other tested models, exhibiting exceptional generalization ability, with coefficient of determination values of 0.9944 and 0.9876 on the testing set, respectively, and significantly lower error measures. With R2 scores above 0.98, Cat Boost and Random Forest also demonstrated high accuracy, indicating dependable performance in identifying nonlinear relationships. Despite having somewhat higher error values than ensemble methods, the Artificial Neural Network (ANN) demonstrated robust approximation capability by achieving competitive results with a high-fidelity correlation of 0.9598 on the testing set. In contrast, Decision Tree and Kernel-based learning algorithms underperformed relative to the ensemble and boosting algorithms, yielding lower R² values (0.8050 and 0.8938, respectively) and higher MSE and MAE values, suggesting limited generalization. Overall, ensemble-based approaches, particularly Gradient Boosting, XGBoost, and CatBoost, outperformed single models by effectively reducing error magnitudes and improving predictive consistency, underscoring their suitability for the given regression task.

These scatter distributions portray the correlation between the experimental (actual) and predicted Material Removal Rate (MRR) values obtained from different machine learning models. The training set predictions are represented by the blue points, and the testing set predictions are represented by the red points. The ideal scenario of perfect prediction, in which the anticipated values precisely match the experimental ones, is shown by the dashed black line.

A close clustering of points along the diagonal line in Figure 6 showcases a strong capacity for consistent inference across diverse input ranges and captures the underlying information corpus distribution with high accuracy (e.g.,

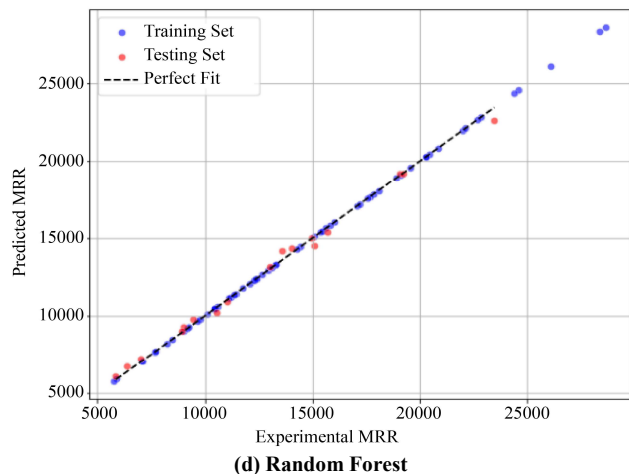
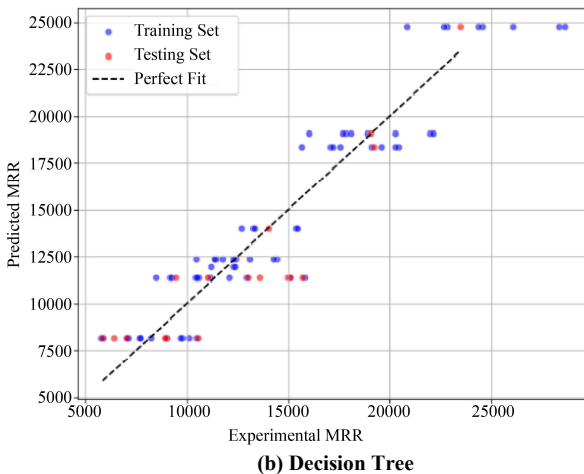
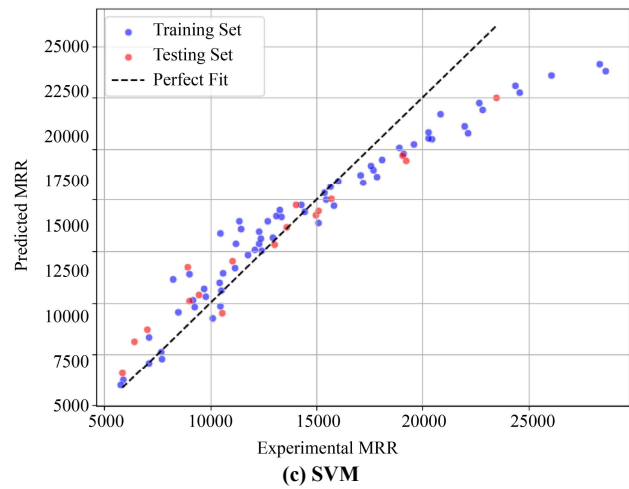
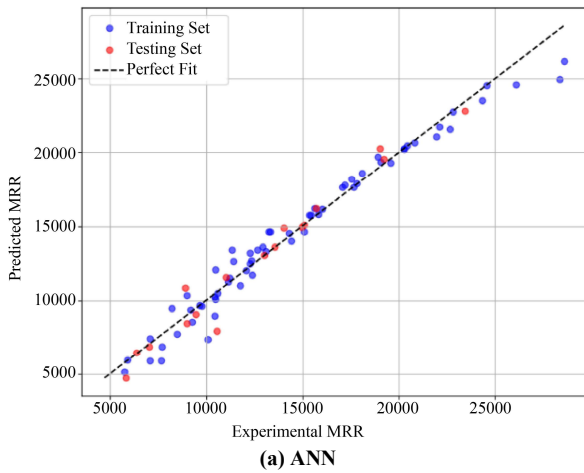
Random forest, CatBoost, Gradient Boost, XGBoost). In contrast, greater deviation from the diagonal line, as seen in the Decision Tree model and Support Vector Machines, highlights weaker predictive capability and higher generalization error. Overall, these graphs provide a comparative visual assessment of model performance, showing which algorithms yield predictions most consistent with experimental outcomes. The synchronicity between the experimental and predicted MRR is visualized in Figure 7. The Gradient Boosting Regressor's projections (orange cross markers) exhibit minimal deviation from the measured observations (blue circular markers) across the entire observation pool.

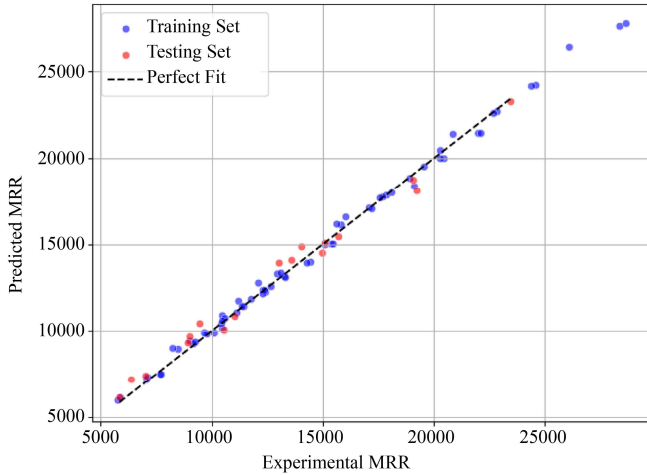
As depicted in the plot, the model-generated estimates closely follow the trend of the actual measurements globally across the sampled population. The marginal residual errors between the two curves reveal a significant trend in the Gradient Boosting model, which effectively discerned the intrinsic correlations, demonstrating its high predictive accuracy.

This observation is consistent with the quantitative metrics, where Gradient Boosting achieved the highest R² score (0.9944) and the lowest errors (MSE = 127,309; MAE = 281.26) among all tested algorithms.

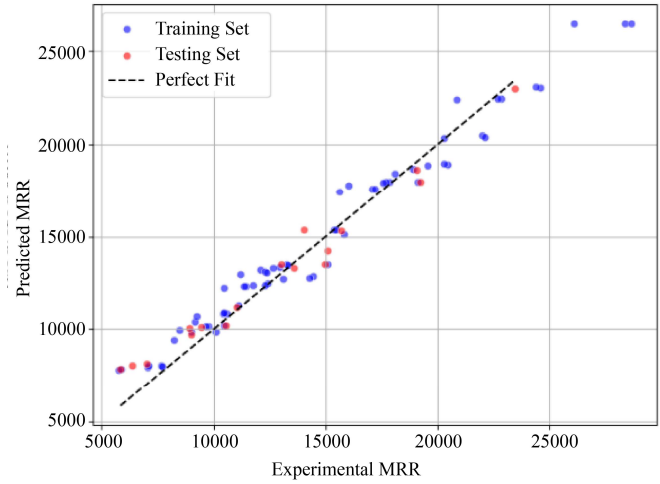
Table 8. Performance measures for MRR prediction

Measure		ANN	Decision Tree	SVM	Random Forest	Adaboost	XGBoost	Gradient Boost	CatBoost
R ²	Training	0.9698	0.8926	0.8527	0.9962	0.9644	0.9999	1.0000	0.9989
	Testing	0.9598	0.8050	0.8938	0.9842	0.9550	0.9876	0.9944	0.9906
MSE	Training	936673	3341109	4581738	117479	1108313	3976	2	33468
	Testing	911881	4423643	2408136	357415	1021603	281887	127309	214095
MAE	Training	678.67	1505.34	1522.29	266.60	852.28	51.14	1.09	147.07
	Testing	645.35	1713.05	1271.51	513.21	866.84	435.88	281.26	399.37

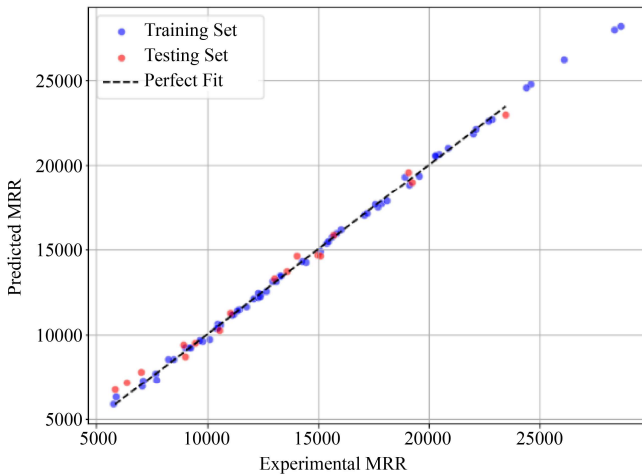




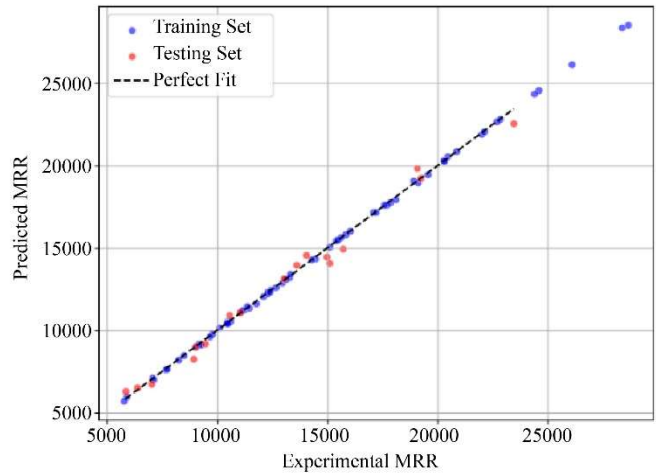
(e) Ada Boost



(g) Gradient boosting



(f) XG Boost



(h) Cat Boost

Fig. 6 Statistical discrepancy analysis between model estimates and experimental trials

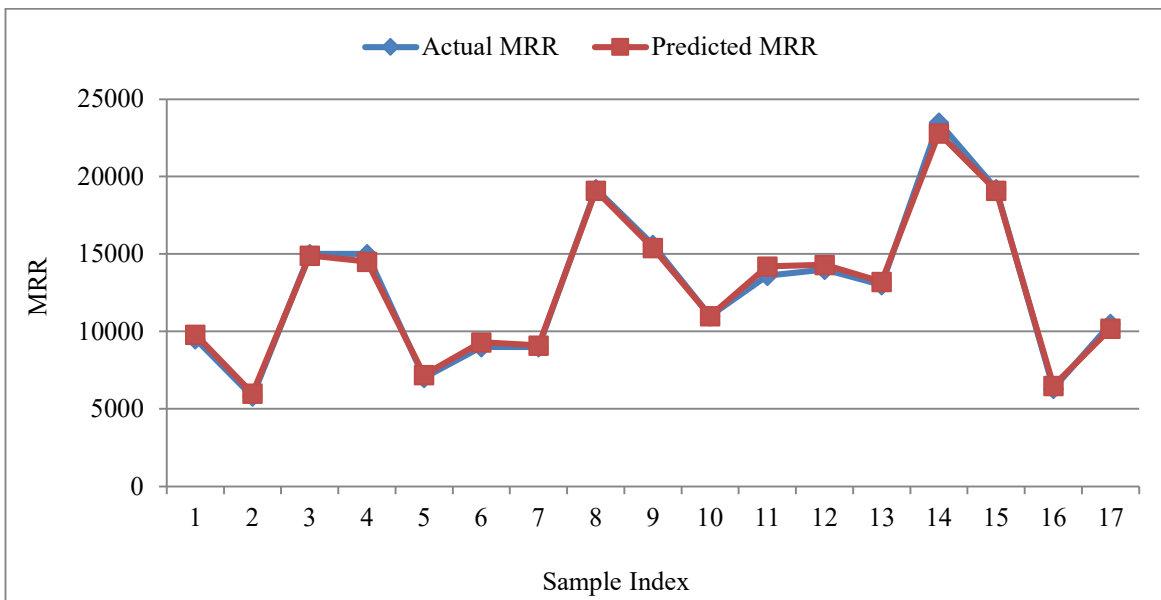


Fig. 7 Comparison of actual and predicted MRR using gradient boosting regressor

5. Conclusion

This study found that using nanofluids made from palm oil can improve machining performance when a small amount of lubricant is used. When we used this method to cut AISI 1040 steel, it went fast, and we were able to remove a lot of material. We think this is because the tiny particles of SiC and TiO₂ in the palm oil helped to cool and lubricate the cutting tool. These particles made it possible to use aggressive machining settings, which made the cutting process smoother. We used a Taguchi L27 orthogonal array to plan 81 tests, which gave us a lot of good data to work with and to make predictions about what would happen in different situations. Artificial Neural Network and seven machine learning models were used to predict the Mean Recession Rate.

The comparison showed that based algorithms, especially Gradient Boosting and XG Boost, did a better job than single models. Gradient Boosting was very good at predicting, with an accuracy of 0.9944, and Boost was also very good, with 0.9876. Artificial Neural Network also did well with 0.9598, which means it is good for making predictions about machining. An Artificial Neural Network is really good for this kind of work. Overall, the findings establish that hybrid nanofluid-assisted MQL not only promotes sustainable and eco-friendly machining but also enhances process efficiency. Furthermore, ensemble learning methods offer powerful predictive capabilities, making them highly applicable for data-driven optimization in modern manufacturing environments. Future work may focus on extending the approach to other machining operations and exploring holistic multi-response refinement to reconcile the competing requirements of minimizing tool degradation and heat generation while maximizing the textural integrity of the processed workpiece.

5.1. Limitations and Future Scope

The results of this study are pretty good. We have to think about some limitations. This project only looked at cutting medium-carbon alloys like AISI 1040 using a technique called microlubrication. So what we found out might not work for ways of cutting metal or for different materials. We also only used three amounts of nanoparticles in our tests. There are some things we did not look at, such as what happens to the nanoparticles over time, whether they clump together, and whether the fluid can be reused. The study on medium-carbon

alloy AISI 1040 has some limitations. Medium-carbon alloys, like AISI 1040, were only tested with microlubrication, which means the results might not apply to metal-cutting processes or materials. We only tested medium-carbon alloys, like AISI 1040, with microlubrication.

The study did not look at medium-carbon alloys like AISI 1040 with cooling methods. We did not test amounts of nanoparticles, only three, in the medium-carbon alloys like AISI 1040.

The medium-carbon alloys, like AISI 1040, are studied in limited ways because they do not consider long-term use or what happens to the fluid after it is used. We looked at how the machine worked by seeing how fast it could remove material. We did not check other important things, such as how the tool wears out, how hot it gets, how well the surface looks, and how much power it uses. When it comes to making models, the Artificial Intelligence (AI) systems were taught using a large amount of data from experiments done in a lab. This might make them not very good at predicting what will happen in a factory where things can vary a lot. The Artificial Intelligence (AI) systems were trained on a large amount of empirical data, which is a problem because it can affect how well they perform in the real world. Artificial intelligence (AI) is not perfect. It needs more data to work better. The framework we have now gives us a starting point to look at how vegetable-oil-based nanocomposites work in multi-point rotational cutting and high-precision grinding. We should try out various kinds of nanoparticles, mix them in various ratios, and see how the shape and amount of particles affect things. This can improve the lubrication and cooling of vegetable-oil-based nanocomposites. We also need to do research on how stable these nanofluids are, how they work with friction, and if they are good for the environment. Vegetable-oil-based nanocomposites are the focus of our work. Furthermore, incorporating a broader array of output characteristics, encompassing cutting-tool degradation, mechanical load variations, thermal gradients, and subsurface metallurgical properties, would facilitate a more rigorous multi-criteria optimization of the machining process. From a data-driven perspective, incorporating real-time sensor data, larger datasets, and advanced approaches such as physics-informed or hybrid machine learning models could significantly improve prediction accuracy and support the development of intelligent and sustainable machining systems.

References

- [1] Ayşegül Çakır Şencan et al., "Evaluation of Machining Characteristics of SiO₂ Doped Vegetable based Nanofluids with Taguchi Approach in Turning of AISI 304 Steel," *Tribology International*, vol. 191, 2024. [[CrossRef](#)] [[Google Scholar](#)] [[Publisher Link](#)]
- [2] Wei Li et al., "Investigation of a Green Nanofluid Added with Graphene and Al₂O₃ Nano-additives for Grinding Hard-to-cut Materials," *Tribology International*, vol. 195, 2024. [[CrossRef](#)] [[Google Scholar](#)] [[Publisher Link](#)]
- [3] Dibya Ranjan Panigrahi, and Gaurav Bartarya Chetan, "Drilling Performance of Nickel-based Hastelloy C276 under Mono and Hybrid Nanofluids Environments," *Journal of Manufacturing Processes*, vol. 120, pp. 1213-1230, 2024. [[CrossRef](#)] [[Google Scholar](#)] [[Publisher Link](#)]

- [4] A.I. Gómez-Merino et al., “Experimental Assessment of Thermal and Rheological Properties of Coconut Oil-silica as Green Additives in Drilling Performance based on Minimum Quantity of Cutting Fluids,” *Journal of Cleaner Production*, vol. 368, pp. 1-15, 2022. [[CrossRef](#)] [[Google Scholar](#)] [[Publisher Link](#)]
- [5] Ahmed Mohamed Mahmoud Ibrahim et al., “Graphene Nanoplatelets-Water Nanofluids: A Sustainable Approach to Enhancing Ti-6Al-4V Grinding Performance through Minimum Quantity Lubrication,” *Tribology International*, vol. 201, 2025. [[CrossRef](#)] [[Google Scholar](#)] [[Publisher Link](#)]
- [6] M. Naresh Babu et al., “Investigation of the Characteristic Properties of Graphene-based Nanofluid and its Effect on the Turning Performance of Hastelloy C276 Alloy,” *Wear*, vol. 510-511, 2022. [[CrossRef](#)] [[Google Scholar](#)] [[Publisher Link](#)]
- [7] Emirhan Saatçi et al., “Orthogonal Turning of AISI 310S Austenitic Stainless Steel under Hybrid Nanofluid-Assisted MQL and a Sustainability Optimization using NSGA-II and TOPSIS,” *Sustainable Materials and Technologies*, vol. 36, 2023. [[CrossRef](#)] [[Google Scholar](#)] [[Publisher Link](#)]
- [8] Hongfei Wang et al., “Suppression Mechanism of Diamond Tool Wear by Graphene Nanofluid in Micro-Milling of TC4 Alloy: A Study Combining Experimental and Molecular Dynamics,” *Journal of Manufacturing Processes*, vol. 115, pp. 310-322, 2024. [[CrossRef](#)] [[Google Scholar](#)] [[Publisher Link](#)]
- [9] Utku Demir et al., “Sustainability Assessment and Optimization for Milling of Compacted Graphite iron using Hybrid Nanofluid Assisted Minimum Quantity Lubrication Method,” *Sustainable Materials and Technologies*, vol. 38, 2023. [[CrossRef](#)] [[Google Scholar](#)] [[Publisher Link](#)]
- [10] Çağrı Vakkas Yıldırım et al., “The Effect of Nanofluids Reinforced with Different Surfactants on the Machining and Friction-wear Properties of Waspaloy,” *Tribology International*, vol. 181, 2023. [[CrossRef](#)] [[Google Scholar](#)] [[Publisher Link](#)]
- [11] Ashutosh Roushan et al., “Wear Behavior of AlTiN Coated WC Tools in Micromilling of Ti6Al4V Alloy using Vegetable Oil-based Nanofluids,” *Tribology International*, vol. 188, 2023. [[CrossRef](#)] [[Google Scholar](#)] [[Publisher Link](#)]
- [12] Zhirong Pan et al., “Cutting Force Model of Milling Titanium Alloy with C60 Nanofluid Minimum Quantity Lubrication,” *Journal of Manufacturing Processes*, vol. 105, pp. 295-306, 2023. [[CrossRef](#)] [[Google Scholar](#)] [[Publisher Link](#)]
- [13] Xuhong Guo et al., “Effect of Magnetic Field on Cutting Performance of Micro-Textured Tools under Fe₃O₄ Nanofluid Lubrication Condition,” *Journal of Materials Processing Technology*, vol. 299, 2022. [[CrossRef](#)] [[Google Scholar](#)] [[Publisher Link](#)]
- [14] Gangqiang Zhang et al., “Effect of SiC Nanofluid Minimum Quantity Lubrication on the Performance of the Ceramic Tool in Cutting Hardened Steel,” *Journal of Manufacturing Processes*, vol. 84, pp. 539-554, 2022. [[CrossRef](#)] [[Google Scholar](#)] [[Publisher Link](#)]
- [15] Tran Bao Ngoc et al., “Influence of Al₂O₃/MoS₂ Hybrid Nanofluid MQL on Surface Roughness, Cutting Force, Tool Wear and Tool Life in Hard Turning,” *Forces in Mechanics*, vol. 16, pp. 1-11, 2024. [[CrossRef](#)] [[Google Scholar](#)] [[Publisher Link](#)]
- [16] Mayur A. Makhesana et al., “Influence of MoS₂ and Graphite-Reinforced Nanofluid-MQL on Surface Roughness, Tool Wear, Cutting Temperature and Microhardness in Machining of Inconel 625,” *CIRP Journal of Manufacturing Science and Technology*, vol. 41, pp. 225-238, 2023. [[CrossRef](#)] [[Google Scholar](#)] [[Publisher Link](#)]
- [17] Şenol Şirin, “Investigation of the Performance of Cermet Tools in the Turning of Haynes 25 Superalloy under Gaseous N₂ and Hybrid Nanofluid Cutting Environments,” *Journal of Manufacturing Processes*, vol. 76, pp. 428-443, 2022. [[CrossRef](#)] [[Google Scholar](#)] [[Publisher Link](#)]
- [18] Kedong Zhang et al., “Study on the Cooling and Lubrication Mechanism of Magnetic Field-Assisted Fe₃O₄@CNTs Nanofluid in Micro-Textured Tool Cutting,” *Journal of Manufacturing Processes*, vol. 85, pp. 556-568, 2023. [[CrossRef](#)] [[Google Scholar](#)] [[Publisher Link](#)]
- [19] Fanning Meng et al., “A Novel Approach of Composite Turning for Compacted Graphite Iron using Minimum Quantity Lubrication and Liquid Nitrogen Jetting by a Developed Setup,” *Journal of Manufacturing Processes*, vol. 117, pp. 278-288, 2024. [[CrossRef](#)] [[Google Scholar](#)] [[Publisher Link](#)]
- [20] Arun Kumar Bambam, and Kishor Kumar Gajrani, “In Pursuit of Sustainability in Machining Titanium Alloys using Phosphonium-based Halogen-free Ionic Liquids as Potential Metalworking Fluid Additives,” *Tribology International*, vol. 199, 2024. [[CrossRef](#)] [[Google Scholar](#)] [[Publisher Link](#)]
- [21] Qinqiang Wang et al., “Prediction and Formation Mechanism of Serrated Chips in Cutting of SA508–3 Steel under Enhanced Cooling and Lubrication Environments,” *Tribology International*, vol. 200, 2024. [[CrossRef](#)] [[Google Scholar](#)] [[Publisher Link](#)]
- [22] Shuncaí Li et al., “Study of Different Cutting Fluids Effect on the Coupling Characteristics of Milling Noise-Vibration and Surface Roughness of TA2 Pure Titanium,” *Journal of Manufacturing Processes*, vol. 118, pp. 103-115, 2024. [[CrossRef](#)] [[Google Scholar](#)] [[Publisher Link](#)]
- [23] Shenliang Yang et al., “Effect of Cutting Fluids on Surface Residual Stress in Machining of Waspaloy,” *Journal of Materials Processing Technology*, vol. 322, pp. 1-50, 2023. [[CrossRef](#)] [[Google Scholar](#)] [[Publisher Link](#)]
- [24] Aswani Kumar Singh, and Varun Sharma, “Sustainable Grinding Approach to Analyze Surface Integrity of Nickel-based Superalloy using Atomized Green Cutting Fluid,” *Journal of Manufacturing Processes*, vol. 102, pp. 1023-1042, 2023. [[CrossRef](#)] [[Google Scholar](#)] [[Publisher Link](#)]

- [25] Amir Alhams et al., “Enhanced Bearing Fault Diagnosis through Trees Ensemble Method and Feature Importance Analysis,” *Journal of Vibration Engineering and Technologies*, vol. 12, pp. 109-125, 2024. [[CrossRef](#)] [[Google Scholar](#)] [[Publisher Link](#)]
- [26] S. Stemmer et al., “Well-Informed Neural Network: An Approach for the Prediction of the Width of Flank Wear Land in Turning Processes,” *Procedia CIRP*, vol. 133, pp. 84-89, 2025. [[CrossRef](#)] [[Google Scholar](#)] [[Publisher Link](#)]
- [27] Hui Liu, Markus Meurer, and Thomas Bergs, “Hybrid Modeling Approach for Predicting Tool Temperature in Metal Cutting Processes,” *Procedia CIRP*, vol. 133, pp. 316-321, 2025. [[CrossRef](#)] [[Google Scholar](#)] [[Publisher Link](#)]
- [28] Nabil Ouerhani et al., “Data-Driven Thermal Deviation Prediction in Turning Machine-Tool - A Comparative Analysis of Machine Learning Algorithms,” *Procedia Computer Science*, vol. 200, pp. 185-193, 2022. [[CrossRef](#)] [[Google Scholar](#)] [[Publisher Link](#)]
- [29] Ahmed B. Khoshaim et al., “Prediction of Residual Stresses in Turning of Pure Iron using Artificial Intelligence-based Methods,” *Journal of Materials Research and Technology*, vol. 11, pp. 2181-2194, 2021. [[CrossRef](#)] [[Google Scholar](#)] [[Publisher Link](#)]
- [30] F.J. Trujillo et al., “Ann-based Predictive Model of Geometrical Deviations in Dry Turning of AA7075 (Al-Zn) Alloy,” *Measurement*, vol. 243, pp. 1-18, 2025. [[CrossRef](#)] [[Google Scholar](#)] [[Publisher Link](#)]
- [31] Andrea Abeni et al., “A Predictive Method for Cumulative Tool Wear in Variable Cutting Speed Turning Operations,” *Procedia CIRP*, vol. 133, pp. 454-459, 2025. [[CrossRef](#)] [[Google Scholar](#)] [[Publisher Link](#)]
- [32] Sampsa Vili Antero Laakso et al., “Hybrid FE-ML Model for Turning of 42CrMo4 Steel,” *CIRP Journal of Manufacturing Science and Technology*, vol. 55, pp. 333-346, 2024. [[CrossRef](#)] [[Google Scholar](#)] [[Publisher Link](#)]
- [33] Yaoxuan Zhu et al., “Data-Driven Approaches for Surface Quality Monitoring and Prediction based on Heterogeneous Multi-Channel Signal Fusion in Hard Part Machining,” *Engineering Applications of Artificial Intelligence*, vol. 160, pp. 1-31, 2025. [[CrossRef](#)] [[Google Scholar](#)] [[Publisher Link](#)]
- [34] Ch Saikrupa, G. ChandraMohan Reddy, and Sriram Venkatesh, “Application of Machine Learning based Algorithm to Predict Performance of Turning Al-SiC-MWCNT using Cryogenically Treated Textured Insert,” *Hybrid Advances*, vol. 10, pp. 1-7, 2025. [[CrossRef](#)] [[Google Scholar](#)] [[Publisher Link](#)]
- [35] Anil K. Srivastava, and Md. Mofakkirul Islam, “Prediction of Tool Wear and Surface Finish using ANFIS Modelling during Turning of Carbon Fiber Reinforced Plastic (CFRP) Composites,” *Manufacturing Letters*, vol. 41, pp. 658-669, 2024. [[CrossRef](#)] [[Google Scholar](#)] [[Publisher Link](#)]
- [36] Lena Geißel, and Petra Wiederkehr, “Bayesian Approach to Determine Force Model Parameters for the Prediction of Cutting Forces in Turning Operations,” *Procedia CIRP*, vol. 117, pp. 378-383, 2023. [[CrossRef](#)] [[Google Scholar](#)] [[Publisher Link](#)]
- [37] Guo Li et al., “Analysis and Prediction of Residual Stresses based on Cutting Temperature and Cutting Force in Rough Turning of Ti-6Al-4V,” *Heliyon*, vol. 8, no. 11, pp. 1-16, 2022. [[CrossRef](#)] [[Google Scholar](#)] [[Publisher Link](#)]
- [38] Jannis Jacob, Markus Meurer, and Thomas Bergs, “Surface Roughness Prediction in Hard Turning (Finishing) of 16MnCr5 Using a Model Ensemble Approach,” *Procedia CIRP*, vol. 126, pp. 504-507, 2024. [[CrossRef](#)] [[Google Scholar](#)] [[Publisher Link](#)]
- [39] Harshal Aher, and Nilesh Ghuge, “Performance Comparison of Machine Learning Algorithms for Condition Monitoring of Tapered Roller Bearings,” *Tribology and Materials*, vol. 4, no. 2, pp. 100-115, 2025. [[CrossRef](#)] [[Google Scholar](#)] [[Publisher Link](#)]
- [40] Qi Li et al., “Fault Diagnosis of Nuclear Power Plant Sliding Bearing-rotor Systems using Deep Convolutional Generative Adversarial Networks,” *Nuclear Engineering and Technology*, vol. 56, no. 8, pp. 2958-2973, 2024. [[CrossRef](#)] [[Google Scholar](#)] [[Publisher Link](#)]